2014

Computational Investigation of Injectable Treatment Strategies for Myocardial Infarction

Hua Wang
University of Kentucky, hwa229@g.uky.edu

STUDENT AGREEMENT:

I represent that my thesis or dissertation and abstract are my original work. Proper attribution has been given to all outside sources. I understand that I am solely responsible for obtaining any needed copyright permissions. I have obtained needed written permission statement(s) from the owner(s) of each third-party copyrighted matter to be included in my work, allowing electronic distribution (if such use is not permitted by the fair use doctrine) which will be submitted to UKnowledge as Additional File.

I hereby grant to The University of Kentucky and its agents the irrevocable, non-exclusive, and royalty-free license to archive and make accessible my work in whole or in part in all forms of media, now or hereafter known. I agree that the document mentioned above may be made available immediately for worldwide access unless an embargo applies.

I retain all other ownership rights to the copyright of my work. I also retain the right to use in future works (such as articles or books) all or part of my work. I understand that I am free to register the copyright to my work.

REVIEW, APPROVAL AND ACCEPTANCE

The document mentioned above has been reviewed and accepted by the student's advisor, on behalf of the advisory committee, and by the Director of Graduate Studies (DGS), on behalf of the program; we verify that this is the final, approved version of the student's thesis including all changes required by the advisory committee. The undersigned agree to abide by the statements above.

Hua Wang, Student

Dr. Jonathan Wenk, Major Professor

Dr. James McDonough, Director of Graduate Studies

COMPUTATIONAL INVESTIGATION OF INJECTABLE TREATMENT STRATEGIES FOR MYOCARDIAL INFARCTION

THESIS

A thesis submitted in partial fulfillment of the requirements for the degree of Masters of Science in Mechanical Engineering in the College of Engineering
at the University of Kentucky

By

Hua Wang

Lexington, Kentucky

Director: Dr. Wenk, Professor of Mechanical Engineering

Lexington, Kentucky

2014

ABSTRACT OF THESIS

COMPUTATIONAL INVESTIGATION OF INJECTABLE TREATMENT STRATEGIES FOR MYOCARDIAL INFARCTION

Heart failure is an important medical disease and impacts millions of people throughout the world. In order to address this problem, treatments that use biomaterial injected into the myocardium of the failing left ventricle are currently being developed. Through this treatment, the biomaterial injections can reduce wall stresses during the cardiac remodeling process. By using computational techniques to analyze the effects of a treatment involving the injection of biomaterial into the left ventricle after myocardial infarction, the material parameters of the hydrogel injections can be optimized. The results show that the hydrogel injections could reduce the global average fiber stress and the transmural average stress seen from optimization. These results indicated that the hydrogel injections could influence the stiffness in passive left ventricle tissue, but there is still need for more research on the active part of ventricular contraction. The conclusion is that hydrogel injection is a viable way to alter ventricular mechanical properties.

KEYWORDS: Finite element modeling, Hydrogel injection, Myocardium infarction, Passive stiffness, Computational optimization

Hua Wang

05/07/2014

COMPUTATIONAL INVESTIGATION OF INJECTABLE TREATMENT STRATEGIES FOR MYOCARDIAL INFARCTION

By

Hua Wang

Dr. Jonathan Wenk

Director of Thesis

Dr. James McDonough

Director of Graduate Studies

05/07/2014

Date

Acknowledgments

It would not have been possible to write this Master's thesis without the help and support of the kind people around me.

Foremost, I would like to express my sincere gratitude to my graduate advisor Prof. Jonathan Wenk, for his excellent guidance, patience and providing me with an excellent atmosphere for doing research, for enlightening me the first glance of research. Special thanks goes to Prof. Keith Rouch and Prof. Brandon Fornwalt who were willing to participate in my final defense committee.

Besides, I would like to thank my labmates in Computational Biomechanics Laboratory: Dimitri Mojsejenko, Xiaoyan Zhang and Amir Nikou, for the stimulating discussions and all the fun we have had in the last two years.

Finally, I would like to thank my parents and my boyfriend, they were always supporting me and encouraging me with their best wishes, also cheering me up and stood by me through the good times and bad.

TABLE OF CONTENTS

LIST OF TABLES

LIST OF FIGURES

CHAPTER 1

Background

Myocardial infarction

As the American Heart Association Statistic reported in 2011, cardiovascular disease is the leading cause of death in the United States, nearly 2200 die each day. And estimated 82.6 million American adults (>1 in 3) have 1 or more types of cardiovascular disease. In state of Kentucky, more than 40% adults have multiple risk factors. In terms of economic impact, the total cost due to cardiovascular disease exceeded $286 billion. It has been reported that more than a million people in the United States have a myocardial infarction (MI) each year. About half (515,000) of these people die as a result. About one-half of those who die do so within one hour of the start of symptoms and before reaching the hospital. Even though heart failure is a significant medical burden to the developed world, there remains a need for better solutions to solve this problem. Before using modeling methods, the only way to observe MI is doing experiment. Now we can use finite element methods (FEM) to build the model of heart, so that it can reduce the cost and times of experiments. To solve this problem, a novel method called “Intra-myocardial biomaterial injection therapy” showed up in recent years. It can help patient to treat the heart disease [1]. The biomaterial injection can reduce the stress of the failing ventricular wall and act to retard the progression of heart failure. This method is based on the FEM model to observe the stress changed in the ventricular wall.

There are several models that can be used to represent the passive mechanical behavior of the left ventricle (LV). Certain models can also capture important detailed properties of heart failure. Some investigated influences include the constitutive nonlinear interactions between the responses in myocardium tissue to different loading patterns, the influences of the structure of laminar myofibre sheet, the effects of transverse stresses developed by the myocytes and the relationship between the architecture of collagen fibre and mechanical behavior in healing scar tissue after MI [2]. For example, isotropic models were developed by Demiray in 1976 [3]. For transversely isotropic models, Humphrey et al. construct a pseudostrain-energy function to determine the relation of passive cardiac tissue [4]. Guccione et al. developed a transversely isotropic model and predicted that the fiber strain curves generated from the model agreed closely with experimental data. Additionally, they showed that fiber structure can alter the stress in the endocardium in the passive LV, torsion, residual stress and material anisotropy [5]. Costa et al. also used transversely isotropic models to analyze mechanics behavior in large-scale anatomical models [6]. Recently, orthotropic models could help researchers to analyze more details about the orthotropic properties of myocardium. In 2001, Costa et al. reported that the constitutive properties of myocardium were three dimensional, anisotropic, nonlinear and time dependent. Based on these properties, they demonstrated orthotropic models in the study of MI [2].

Morphology and structure

The structure of heart is quite complicated. In a human, the size is almost like a person's fist, and yet it plays as a crucial role in a body. The mass of a human's heart is

between 250-350 grams. It is located anterior to the vertebral column and posterior to the sternum. The heart consists of four chambers, namely the right atria, which receives oxygen-poor blood from the body, the right ventricle, which pumps blood into the lungs, the left atria, which received oxygen-rich blood from the lungs, and the LV, which pumps blood into the body [7]. The structure of heart was shown in figure 1.

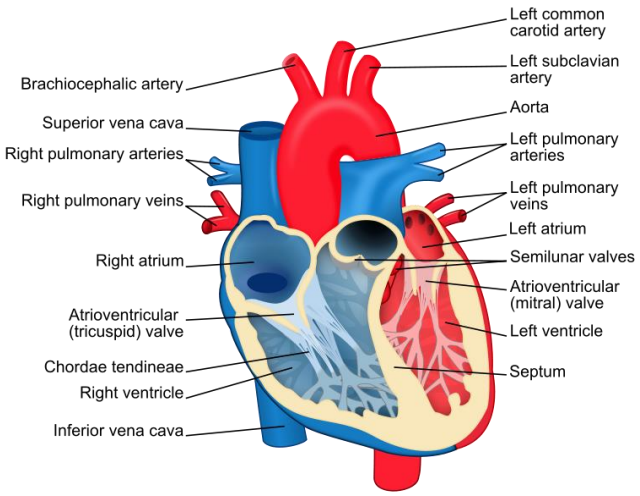

Figure 1 the structure of heart

The wall of human heart can be considered as composed of three major layers, epicardium, myocardium and endocardium. The endocardium lines the inside of the four chambers and it is a serous membrane, with approximate thickness 100 μm, consisting mainly of epimysial collagen, elastin and a layer of endothelial cells, the latter serving as an interfacial layer between the wall and the blood [7].

The fiber orientation in myocardium has been studied for many years. The distribution of stress in the LV wall is impacted by both the fiber tension and fiber orientation. In 1969, the paper by Streeter et al. [8] indicated that the myocardium wall has a well-ordered distribution of fiber varying from -60° to 60° (from epicardium to

endocardium), relative to the circumferential direction, in normal heart. Besides this, in comparison to normal heart, the fiber angles changed in pressure-overload heart. As mentioned in Carew et al. [9], the fiber angle was tested between -67.5° and -90° in endocardium and ranged from 67.5° to 90° in epicardium. The methods used to study the fiber orientations are described in detail the papers [8, 9].

Treatment Methods

Methods to treat MI vary. In 2006, a work done by Wall et al. utilized a finite model to evaluate the effect on cardiac wall stress of injecting non-contractile biomaterial injections into the LV wall [1]. As in previous work by Guccione et, al., they used finite element models to simulate the volume change in the LV cavity. It was shown that the relationship between the stroke volume and stresses in end-diastole state are affected by the local fiber orientation [10]. There are many treatments involving the use of cardiac restraint devices. For instance, the CorCap (Acorn Cardiovascular Inc.) uses Dacron wraps (Figure 2), and the Heart Net (Paracor Medical Inc.) uses nitinol wraps to provide ventricular support during heart failure [11-13]. Other companies, such as the Myosplint (Myocor Inc.), provide interior ventricular support to address dilation from heart failure. The primary goal of each of these devices is to reduce the stress in the ventricular wall during heart failure. Myosplint uses their device to change the geometry of the LV and reduce the burden in dilated cardiomyopathy [14, 15].

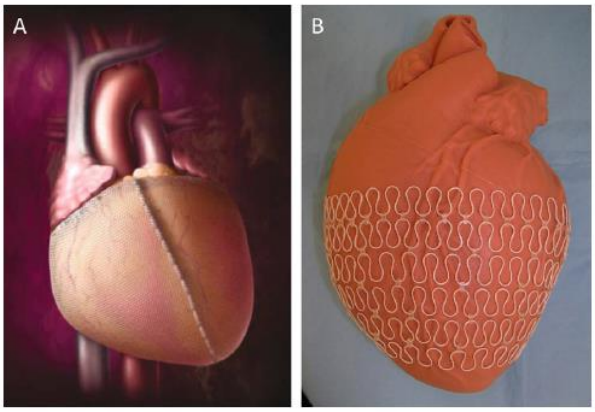

Figure 2 Cardiac restraint devices. (A) Dacron woven mesh (B) Elastic nitinol metal wrap. (From Blom et all. [16] and Klodell dt all. [17])

To treat heart failure, injections made of biomaterial can be used to reduce the stress in LV wall. In Kichula et al. [17] a new method combined experimental and computational techniques to estimate the mechanical properties after the hydrogel injection in normal myocardium. In order to determine how injectable volume and mechanical parameters influence myocardium wall, experimental measurements were first used to obtain hydrogel injection volumes by magnetic resonance imaging (MRI). Subsequently, biaxial testing of tissue sample was performed. Finally, based on the observation from experimental measurements a constitutive model was used to fit parameters to ex vivo samples of myocardium. This method was used to mimic the response of the injected myocardium by building finite element models that used those properties. The results indicated that biomaterial could be used to reduce the wall stress during the LV remodeling.

Constitutive behavior

The material behavior of active and passive myocardium is considered as hyperelastic, incompressible, and transversely isotropic [5, 18]. The relationship used to describe myocardium mechanics by the strain energy function, W, is shown below. These properties were assigned as the material parameters in the finite element model. This model is a phenomenological model, which is transversely isotropic with respect to the local fiber direction [5].

$$W = \frac{C}{2}[\exp(Q) - 1] \quad \text{(Eq 1)}$$

$$Q = b_f E_{11}^2 + b_t(E_{22}^2 + E_{33}^2 + E_{23}^2 + E_{32}^2) + b_{fs}(E_{12}^2 + E_{21}^2 + E_{13}^2 + E_{31}^2) \quad \text{(Eq 2)}$$

Where E_{11} is strain in fiber direction, E_{22} is strain in cross-fiber direction, E_{33} is radial strain transverse to the fiber direction, and the rest are shear strains, and C, b_f, b_t, and b_{fs} are the diastolic material parameters [17].

Systolic contraction can be modeled as the sum of the passive stress derived from the strain energy function and active fiber directional component T_0 [19]. T_0 is a function of time (t), peak intracellular calcium concentration (Ca_0), sarcomere length (l) and maximum isometric tension achieved at the longest sarcomere length (T_{max}) [18].

$$S = pJC^{-1} + 2J^{-2/3}\, Dev\left(\frac{\partial \widetilde{W}}{\partial C}\right) + T_0\{t, Ca_0, l, T_{max}\} \quad \text{(Eq 3)}$$

where S is the second Piola-Kirchoff stress tensor, p is the hydrostatic pressure, J is the Jacobian of the deformation gradient tensor, C is the right Cauchy-Green deformation tensor, and Dev is the deviatoric projection operator [20].

C and B depend on the deformation gradient F, and are defined by

$C = F^T F$ and $B = FF^T$ (Eq 4)

$\text{Dev}(\cdot) = (\cdot) - \frac{1}{3}([\cdot]:C)C^{-1}$ (Eq 5)

$\widetilde{W}$ is isochoric contribution of the strain energy function.

$W = U(J) + \widetilde{W}(\tilde{C})$ (Eq 6)

Where U is the volumetric contribution.

At end-systole state, the active fiber directional stress component is defined by a time-varying elastance model which is reduced to [21]

$$T_0 = \frac{1}{2} T_{max} \frac{Ca_0^2}{Ca_0^2 + ECa_{50}^2} \left(1 - \cos\left(\frac{0.25}{ml_R\sqrt{2E_{11}+1}+b} + 1\right)\pi\right) \quad \text{(Eq 7)}$$

where m and b are constants, and ECa_{50}^2 is the length-dependent calcium sensitivity given by,

$$ECa_{50}^2 = \frac{(Ca_0)_{max}}{\sqrt{exp\left[B\left(l_R\sqrt{2E_{11}+1} - l_0\right)\right] - 1}} \quad \text{(Eq 8)}$$

where B is a constant, $(Ca_0)_{max}$ is maximum peak intracellular calcium concentration, l_0 is the sarcomere length at which no active tension develops, and l_R is the stress-free

sarcomere length [19]. The material properties of active myocardium can be found in [22].

Mechanical behavior of the passive myocardium

The passive myocardium mechanical behavior plays a significant role in understanding myocardium infarction. Most of our preliminary knowledge of the mechanical behavior of the passive myocardium was originally from uniaxial test on papillary muscles or trabeculae carnae [23, 24]. After several years, people found that uniaxial test cannot describe the multi-axial behavior of the passive myocardium. Biaxial test was reported by Demer and Yin to investigate the anisotropic behavior of passive myocardium [25]. They determine passive myocardium mechanical properties in canine myocardium. Non-linear elasticity and viscoelasticity with strain-rate dependence in the stress-strain relations were found under biaxial testing in passive myocardium [25]. Later Yin et al. reported that myocardium is consistently stiffer in the direction of the muscle fibers than it is in the orthogonal cross-fiber direction [24].

During biaxial testing, the Cauchy stress can be defined as:

$$\sigma_{11} = \frac{C}{2} e^{\frac{b_f}{4}(\lambda_1^2-1)^2+\frac{b_t}{4}\left((\lambda_2^2-1)^2+(\frac{1}{\lambda_1^4\lambda_2^4}-1)^2\right)} \left(b_f(\lambda_1^4-\lambda_1^2) - b_t\left(\frac{1}{\lambda_1^4\lambda_2^4}-\frac{1}{\lambda_1^2\lambda_2^2}\right)\right) \quad \text{(Eq 9)}$$

$$\sigma_{22} = \frac{C}{2} e^{\frac{b_f}{4}(\lambda_1^2-1)^2+\frac{b_t}{4}\left((\lambda_2^2-1)^2+(\frac{1}{\lambda_1^4\lambda_2^4}-1)^2\right)} \left(b_t\left(\lambda_1^4-\lambda_1^2-\frac{1}{\lambda_1^4\lambda_2^4}+\frac{1}{\lambda_1^2\lambda_2^2}\right)\right) \quad \text{(Eq 10)}$$

where σ_{11} and λ_1 are the stress and stretch ratio in the circumferential (myofiber) direction, respectively, and σ_{22} and λ_2 are the stress and stretch ratio in the longitudinal (cross-fiber in-plane) direction, respectively. The stretch ratios and normal components of Green-Lagrange strain are related by $E_{ii} = \frac{1}{2}(\lambda_i^2 - 1)$, where i=1,2,3.

CHAPTER 2

Study 1: Effects of Hydrogel Injection on Health Myocardium

Despite advances in FE models of injection treatment, there has yet to be direct comparison between experimental results and models to better understand how materials can influence stress behavior after injection. In the current investigation the focus was on the experimental generation of injection volume/shape data in LV explants using magnetic resonance imaging (MRI) and their mechanical properties using biaxial testing. The biomaterial hydrogel injections used in this study were made of methacrylated hyalutonic acid (MeHA).The experimentally measured information was then employed directly in a FE model of an LV treated with an injection distribution pattern that was previously explored in an in-vivo study, to investigate stress levels based on experimentally derived, rather than theoretical input values. This investigation will ultimately provide a better understanding of the relationship between injectable material properties (i.e., mechanics and volume) and stress reduction post-MI and insight on material design criteria for injectable biomaterials to attenuate LV remodeling. The work presented in this section was done in collaboration with the Burdick Lab at the University of Pennsylvania.

Methods

Non-Contrast Magnetic Resonance Imaging (MRI)

Hydrogel distribution and volume within the myocardium was assessed by mimicking the experimental *in vivo* work of Ifkovits et al.[26]. The research team at UPenn obtained ovine hearts from a local butcher shop. Three minutes after mixing of the MeHA with initiators, 0.3 mL of the hydrogel formulation [4 wt% MeHA, 5Mm APS/TEMED in phosphate buffered saline (PBS)] was injected into the explanted ovine LV myocardial tissue. After 30 minutes, treated samples (hydrogel injected into myocardium tissue) were obtained from the heart within the region from the epicardium to endocardium. After 30 minutes, the tissue with hydrogel material injected was fixed in 4% formalin overnight and paraffin embedded by using standard histological techniques. Injected explants were imaged using MRI without contrast agents by adjusting image parameters to exploit material intrinsic properties; a spin echo pulse sequence was employed and the echo time (30-60 ms) was adjusted for optimal contrast. Voxel size was also altered (0.234 x 0.234 x 1.00 mm^3 vs. 0.234 x 0.234 x 0.234 mm^3) to optimize resolution.

Biaxial Testing

Biaxial testing is a useful way to obtain two-dimensional mechanical behavior. Previous uniaxial testing has demonstrated fiber stress-strain relationship in one direction. According to Walker et al. finite element analysis with only uniaxial contraction stress is insufficient to model the mechanical behavior in myocardium tissue [27]. However, the mechanical behavior of myocardium tissue has two direction (fiber direction and cross-

fiber direction) to calculate. Biaxial testing is used to avoid the limitation of the uniaxial testing. To characterize the mechanical behavior of myocardium tissue, biaxial testing was employed to identify the two directions stress-strain relationship specifically. Biaxial test has been used previously for test infarct material properties [28].

In the current study, injected explant tissue and untreated myocardium samples were prepared and a total of 5 samples were tested per group. Samples were collected from the mid-myocardial region and trimmed to ~7 x 7 mm^2 with a thickness of ~2 mm. Average thickness values were calculated to compute cross-sectional areas in order to determine the stress in each loading directions. The samples were speckle-coated with Verhoeff's stain. Also, samples were equilibrated for ~1 h in PBS at RT. Biaxial test requires the free expansion of the sample edges, thus finger-like grips were made out of waterproof sandpaper (T214 Norton) (~75 x 5 mm^2) to accomplish this [29]. Grips were painted white to enhance contrast and glued (Locite 454). Brass 0.5 mm markers were painted black to enhance contrast. The black makers used to track the strain during the biaxial test process (Fig 3). Three 25 x 1 mm "fingers" were put at the free end so that 6 "fingers" were formed (3 on the top and 3 on the bottom) [17]. Testing was performed by grip-to-grip strain control; all samples were preconditioned, exposed to a 1 hour hold, and then tested. Preconditioning included prestraining to 0.01 equibiaxial strain and then equibiaxially straining to 0.20 for 5 cycles at 0.10 strain/min. The test protocol was identical to the preconditioning parameters; data and images from the final loading curve of each test were used for experimental data analysis.

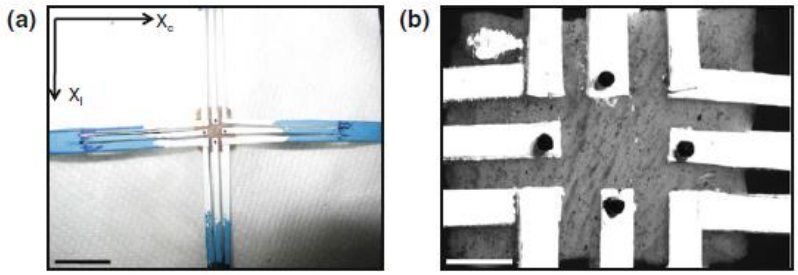

Figure 3 Representative biaxial testing preparation sample.

Stress and strain data obtained from biaxial testing were used to estimate the nonlinear material parameters for building the finite element model. To obtain the tissue strain data, 2-D displacement maps were rendered using the speckle-coated surface via digital image correlation (Vic2D 2009, Correlated Solutions). The basic deformation variable for the description of the local kinematics is the deformation gradient F; and for an incompressible material, there is a constraint on J, where

$$J = \det F \equiv 1 \qquad \text{(Eq 11)}$$

Associated with F are right and left Cauchy-Green tensors C and B.

C and B are defined by

$$C = F^T F \text{ and } B = FF^T \qquad \text{(Eq 12)}$$

Also important for what follows is the Green-Lagrange (or Green) strain tensor, defined by

$$E = \frac{1}{2}(C\text{-}I) \qquad \text{(Eq 13)}$$

Where I is the identity tensor.

The gradient F was calculated in both the longitudinal and circumferential directions from the displacement map of each image by finding the least-squares solution with a Matlab algorithm developed and described by Szczesny et al [30].

Finite Element model

In order to determine the influence of hydrogel injections on myocardial wall stress, two different FE models were built, one with hydrogel injections and one without. FE models were modified from Wenk et al [19]. The wall thickness was approximately 1.3 cm near the equator of the LV and 0.8 cm near the apex. The inner diameter of the endocardial wall near the equator was 4 cm. The myocardium had fiber orientation that varied transmurally in the wall tissue. The angle assigned from epicardium to endocardium was -37° to 83°, respectively. The model was assigned 20 hydrogel injections around the free wall. The number of regions was based on work by Ifkovits et al.[31], where the 20 hydrogel injections were put into an ovine anteroapical infarct region. The resulting finite element models for the current study are shown in Figure 4. The pattern of 5 circumferential by 4 longitudinal injections were assigned in the region of the LV free wall (i.e., no injections in the septum). In the model, the blue part represents injections and the red part the myocardium tissue. The shape of hydrogel injections were modeled as ellipsoidal, and the material properties in these regions were assumed to act like a composite material, i.e, the injection sites were a combination of myocardium and the hydrogel polymer. The shape and volume of the injections was based on the MRI of injected explant tissue.

According to Holmes et al.[32], the passive properties of the myocardium begin to stiffen four to six hours after MI. Since the model was built to mimic the initial time frame after myocardium infarction, it was assumed that the myocardial properties were unchanged. Therefore, the remote region properties were created as same as the properties in the control case biaxial results. The material properties of the hydrogel injection tissue region were obtained from the experimental biaxial testing of samples taken from the center of the ellipsoidal composite site (Fig 4). Since each injection was 0.3 mL, the total amount of volume added to the myocardium wall was 6 mL. The wall thickness was increased to 1.4 mm. Compared to the control case model, the longitudinal dimensions were not changed. The b_{fs} value was set to 12, and it was determined from the literature [27].

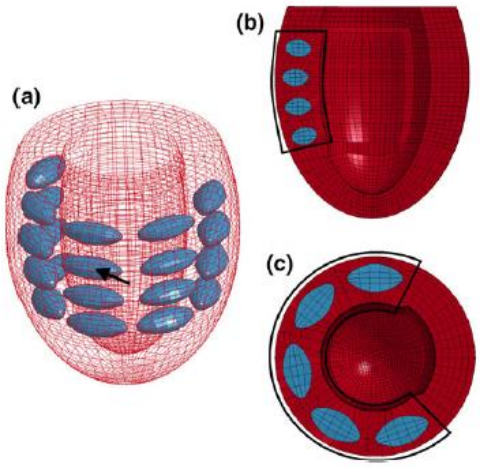

Figure 4 Captured from LS-PrePost (Livemore Software Technology Corporation, Livemore, CA)

Results

Non-contrast MRI

The proton makeup of a water swollen HA hydrogel is different from that of tissue; thus, when injected into an explant, the endogenous properties of the composite hydrogel/tissue region are different compared to tissue alone. It is not completely understood how much of this is due to changes in proton density or relaxation times, yet hydrogels are detectable without the inclusion of contrast agents. Initial studies were performed to understand whether the injected macromer would be present in the tissue, if it is not crosslinked into the gel. To address this, MeHA was injected into explants without initiator and washed for up to 5 days. After 3 days, there were negligible differences between the control tissue and the tissue washed free of macromer (Figure 5). X_c meant circumferential direction and X_l meant longitudinal direction.

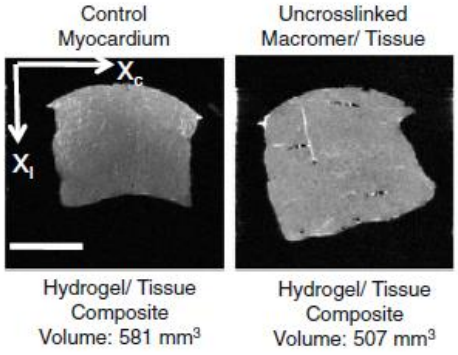

Figure 5 MRI images showed composite in control myocardium and uncrosslinked macromer tissue at day 3.

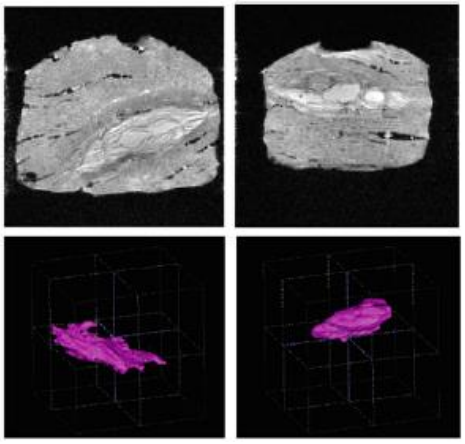

Figure 6 MRI images and 3D images showed tissue with hydrogel injection injected.

The injected composite material was found to spread in the major directions (circumferential, longitudinal, and transmural). The 3-D images could distinguish the composite injection region from the myocardium tissue (Fig 6). The dimensions and volume of hydrogel composite injections were estimated from the MRI data. The average length in circumferential, longitudinal, and transmural directions was found to be 1.725 ± 0.25, 0.575 ± 0.15, and 0.875 ± 0.096 cm, respectively. The volume was calculated as 0.420 ± 0.162 mL, which was larger than the original volume 0.3 mL because of the hydrogel injections dispersing within the tissue. After the hydrogel was injected into the myocardium tissue, it dispersed evenly with the fibers, as could be seen from the figure below, G means hydrogel injection region (Fig 7). The smallest dimension of the hydrogel composite region was in longitudinal direction. This is because the laminar architecture of the fiber sheet in myocardium, the hydrogel injections were dispersed between layers [17].

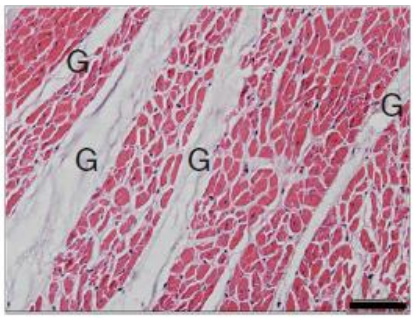

Figure 7 G represents hydrogel injections.

Biaxial testing

Biaxial testing was conducted on 5 control samples and 5 hydrogel composite samples. The curve fit results had a good agreement with experimental data for both control and composite samples. The resulting stress-strain curves were then fit in order to determine the parameters for the constitutive model in Equation 9 and 10. All of the parameters from the curve fitting procedure are reported in Table 1A and 1B for the control and composite case. The average parameters for each case are given in Table 2. The curve fit parameters were plugged into Equation 9 and 10 to generate curves shown in Figure 9. As the figure indicated, the stiffness in composite samples was higher than it in control samples. And the anisotropy was reduced in composite samples compared to control samples. The parameters C, b_f and b_t were determined from the optimization by using genetic algorithm.

Table 1 Biaxial testing results of curve fitting for control (A) and injected region (B).

(A)

Sample #	C (kPa)	b_f	b_t	R^2 (circ)	R^2 (long)
1	0.656	25.44	4.604	0.995	0.995
2	0.817	14.85	1.876	0.988	0.951
3	0.859	28.73	3.217	0.994	0.989
4	0.597	20.20	3.018	0.995	0.965
5	0.470	15.63	4.017	0.988	0.966

(B)

Sample #	C (kPa)	b_f	b_t	R^2 (circ)	R^2 (long)
1	1.179	17.28	9.154	0.996	0.996
2	0.907	8.862	7.731	0.993	0.991
3	0.859	17.87	6.533	0.987	0.970
4	0.484	28.46	4.831	0.981	0.906
5	0.667	15.52	7.527	0.997	0.995

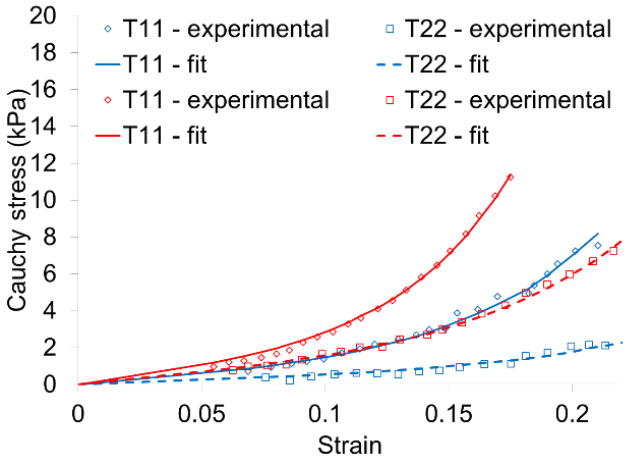

Figure 8 Left: Curve fit results for representative samples of control myocardium and hydrogel/tissuel composite

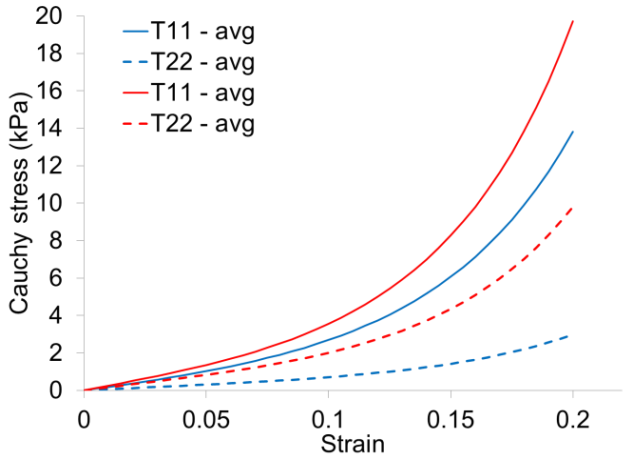

Figure 9 Right: Average curve fit results for representative samples of control myocardium and hydrogel/tissuel composite

Table 2 Average biaxial testing results of curve fitting for control and composite samples.

Case	C (kPa)	b_f	b_t
Control	0.679±0.160	20.97±6.05	3.346±1.04
Composite	0.819±0.262	17.60±7.05	7.155±1.60

In order to see the influences in anisotropy, the "modulus" in different strain ranges was examined. Myocardial physiological stain has been reported to range from 0.1 to 0.15 [31, 33-35].To account for the lower and higher ends, a mechanical assessment was performed between 0.05 and 0.10 and between 0.10 and 0.15 Green-Lagrange strain, where 0.05-0.10 corresponded to the linear toe region in stress-strain curves (Figure 10). Results demonstrated that in longitudinal direction, the moduli of composite samples were higher than in control samples in all Green-Lagrange strain ranges with significant changes at 0.10-0.15. However this trend was not as clear in the circumferential direction. It is well known that healthy normal myocardial tissue is anisotropic, where stiffness in circumferential direction is higher than in longitudinal direction. Overall the results shown the stiffness increased more in the longitudinal direction than it in the circumferential direction. As a result, the anisotropy ratio for the composite tissue was decreased compared to control myocardium. It means stiffening in an anisotropic manner enhanced the influence of hydrogel treatment in decreasing stress.

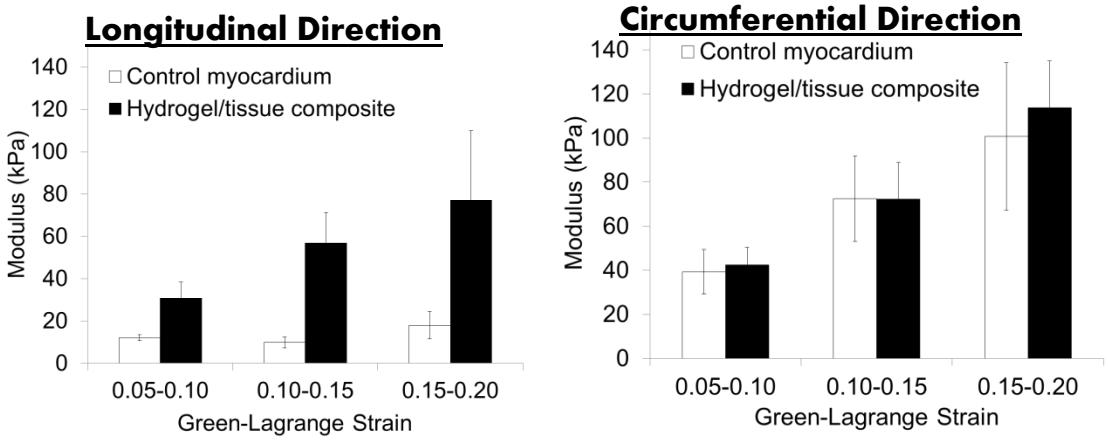

Figure 10 Calculated moduli from tissue strain for control and composite samples in longitudinal direction (left) and circumferential direction (right).

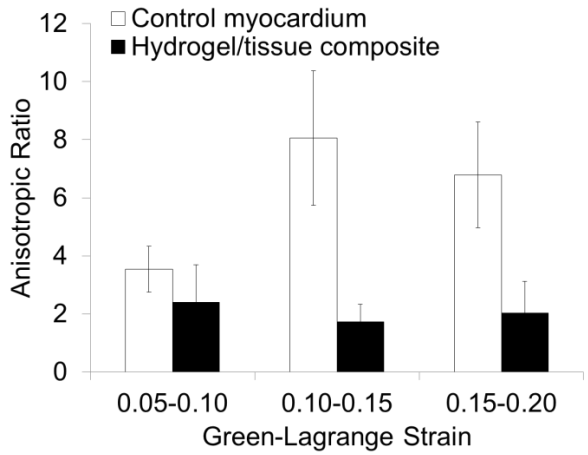

Figure 11 Calculated anisotropic ratio.

Finite element model simulation

All of the cases were run on either a 12-core or 32-core computer node. To compare the influences between injected explant and baseline sample, two models were built, one with injections and one without injections. Both models used the material parameters obtained from biaxial testing. End-diastole stress in different regions in FE model were calculated. As the results shown below, the global average of fiber stress was reduced by roughly 14% due to the presence of the injections. The transmural average, which represents a local change in stress was reduced by 26%. In order to assess the influence of mechanical properties verses wall thickening, since hydrogel injection induced both, simulations were conducted where the properties of the composite regions were assigned to be the same as the control myocardium. Therefore only wall thickening effects altered the stress distribution. It can be seen that the reduction in stress is 10.4% for the global average and 19.9% for the transmural average. Thus, increased stiffness,

due to the hydrogel injection, reduced the stress more than just thickening the ventricle wall alone. The influence of altering the anisotropy of the injection region was explored. This provides insight that could be used to tune the development of the hydrogel. When b_t was assigned to be 1, the fiber stress increased by 6%, whereas when b_t was assigned to be equal to b_f, the fiber stress decreased by 11%. That is because of the Poisson's effect. Thus, as cross-fiber stiffness increases (reducing anisotropy) the fiber stress decreases even further.

Table 3 End-diastolic myofiber stress averaged over different regions.

Case	Global kPa (% diff)	Circumferential kPa (% diff)	Longitudinal kPa (% diff)	Transmural kPa (% diff)
Control	2.89	3.35	3.04	3.37
Composite	2.49 (-13.9%)	2.75 (-18.1%)	2.38 (-21.9%)	2.49 (-26.0%)
Composite w/ control props	2.59 (-10.4%)	2.85 (-14.9%)	2.48 (-18.4%)	2.70 (-19.9%)

Discussion

This study determined the influence of hydrogel injections within the wall of normal myocardium of the LV. The results indicated that the injected hydrogel increases mechanical stiffness in the longitudinal direction and reduces stress along the fiber direction. Previous studies have reported that hydrogel material could reduce the stress of the LV wall, but they were not considering the interaction of the hydrogel material with myocardium tissue. Kortsmit et al, performed a study where the distribution of hydrogel in the infarcted heart was simplified and during their computational study, bulk layers of hydrogel were used to determine the stress reduced in LV wall [36]. In addition, Wenk et al, developed an FE model to defining the injection pattern and material parameters. The results indicated that stress could be reduced during cardiac cycle [19].

In the current study, the biaxial testing results indicated that the injected hydrogel material alters the stiffness of myocardium tissue, generally resulting in a larger mechanical influence in the longitudinal direction than in the circumferential direction compared to control myocardium. The results reported in Figure 10 support the trend that normal myocardial tissue is anisotropic, however, when compared to control samples, composite tissue resulted in decreased anisotropy (Fig 11).

This study also indicated that the hydrogel composite injections increase the stiffness of the myocardium/hydrogel composite region along cross-fiber direction when compared to control myocardium, and also reduce the global average stress along the fiber direction. . It was found that increasing wall thickness, due to the injections, can

reduce stress even if the stiffness was not altered. However, when the cross-fiber stiffness was increased, this led to the largest decrease in fiber stress.

Overall this approach could predict further reduction by changing the formulation of materials and material properties. There are a wide range of materials that have been injected into myocardium and with some systems there is tenability in properties. For instance, by altering the stiffness of the formulation, the stress may be reduced more. This study showed that a formulation that is stiffer overall could further reduce stress. One limitation of the current study is that it only used data on the passive stiffness due to hydrogel injections in LV. The contractility in the injection region was not assessed. The other limitation is that this study should be used in a beating heart instead of an explanted heart. Further research is needed to study the active part during heart contraction in a living LV.

CHAPTER 3

Study 2: Effects of Hydrogel Injection on Myocardial Infarction

Method

This study was performed using Hydroxy-ethyl methacrylate functionalized hyaluronic acid (HeMA-HA) hydrogels, which were injected into a MI. In this study, the hydrogel was functionalized to exhibit controlled and tunable mechanics and degradation once cross-linked, in an attempt to assess the temporal dependency of mechanical

stabilization in LV remodeling [37]. This study was aimed to determine the influences of hydrogel injection on in-vivo properties. During this study, data was used from pigs that underwent ligation of the coronary artery to create MI. Magnetic resonance images (MRI) of LV were collected at 1 weeks, 4 weeks, and 8weeks post MI, where end-diastole pressure and volume were obtained. Endocardium and epicardium surface data were used to generate finite element models for each case. By using the mesh generator TrueGrid, finite element models with experimental surface data were built. After this, Matlab was used to assign the fiber angles to the finite element model in the remote myocardium. The optimization software LS-OPT was used to adjust the material parameters and infarct fiber angles in the FE model and run the simulations.. The optimization was used to compare the FE predicted strain and volume to that measured from MRI. The "best" result was the set of material parameters and MI fiber angles that minimized the difference between the experimental measurement and simulation output. The work presented in this section was done in collaboration with the Burdick Lab and Gorman Lab at the University of Pennsylvania.

MRI

To measure 3D strain in myocardium, the 3D SPAMM MRI tissue-tagging sequence and a 3D optical flow method were used in this study [38]. In previous studies, 2D analysis techniques with optical flow method has been used to estimate LV deformation from tagged CMR images. This method has limited ability to precisely capture the complex radial, circumferential and longitudinal motion associated with normal and diseased

hearts [39, 40]. The 3D analysis technique is a deformable model which fit to either the tag line material points extracted from the image date. Another method used for tagged CMR analysis called harmonic phase method (HARP), which uses tag phase to estimate the underlying tissue displacements [41]. However, this was not used in this study.

Ten custom 2mm platinum makers were sutured to the epicardium around the infarct periphery immediately following infarct induction to enable infarct localization in subsequent MRI acquisitions and post-processing. For regional strain measurements from 3D SPAMM images, infarct boundaries were identified using the previously placed platinum epicardial makers and comparing to landmarks on late-gadolinium enhanced (LGE) images (Fig 12). LGE images could show infarct region more clearly. Detailed 3D deformation patterns derived from the heart of sample pig were illustrated in the figures below. Figure 13 represented phase 1-4 from the sample PMR120 at one week. Figure 14-15 showed the endocardium and epicardium boundaries, as well as the normal region compared to infarct region. Strain data was obtained from end-diastole because during that time there was less noise than the other time points. Too much noise could disturb the images and make them not clear.

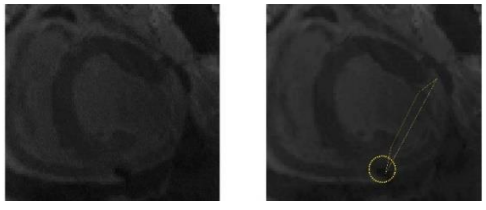

Figure 12 PMR120 1week S12 LGE and S12 LGEMarkers

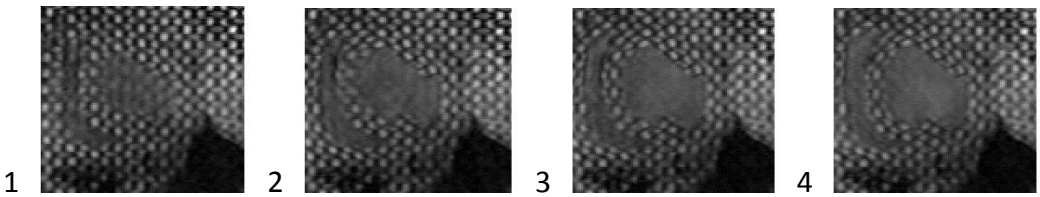

Figure 13 PMR120 1week S16 phase 1-4

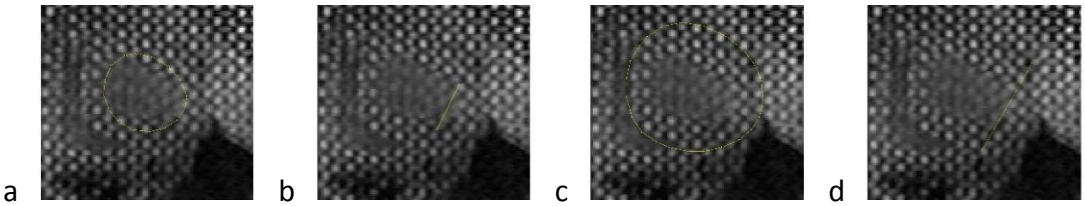

Figure 14 a) PMR120 1week S16 Endocardium. b) PMR120 1week S16 Endocardium Infarct. c) PMR120 1week S16 Epicardium. d) PMR120 1week S16 Epicardium infarct.

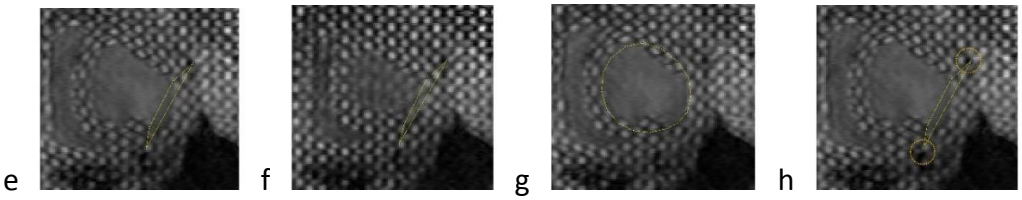

Figure 15 e) PMR120 1week S17 Phase4 Infarct. f) PMR120 1week S16 Infarct. g) PMR120 1week S16 End-diastole phase. h) PMR120 1week S17 Phase4 Infarct Markers

Six control cases (PMR132, PMR134, PMR119, PMR120, PMR135, and PMR137) and nine treated cases (PMR124, PMR126, PMR128, PMR129, PMR130, PMR131, MEP13, MEP17 and MEP19) were used in this study. PMR and MEP were the animal IDs. Experimental data was obtained from pigs that underwent ligation site of the coronary artery to create a posterolateral-MI (Fig 16). For infarct induction, pigs were anesthetized and the LV free wall exposed through a left thoracotomy. Pigs were monitored with electrocardiography throughout the procedure. A posterior MI was induced by suture ligation of the left circumflex artery (LCX) and select obtuse marginal (OM) branches. In nearly all cases, this pattern of coronary ligations produces an infarct comprising 20-25%

of the LV [42]. MRI compatible, thin platinum wire markers were placed on the heart to outline the infarct area. Tracking these markers enabled quantitative assessment of infarct area expansion over time. Thirty minutes post-MI, control pigs received twenty 0.3 mL injections of saline. The treatment cases were given twenty 0.3 mL injections of the hydrogel. Real time 3D echocardiographs and hemodynamic data were obtained at baseline, immediately prior to MI, 30 minutes post-MI, and 30 minutes post injection (Fig 19). MRI scans were performed 5-7 days prior to MI (baseline) and at 1, 4, 8 and 12 weeks post-MI. For each MRI scan, a pressure transducer was guided into the LV for cardiac gating. Cardiac MRI was used to noninvasively assess global and regional cardiac structure and function through a series of three scans: 1) cine imaging to assess global and regional morphology, 2) delayed contrast enhancement (DCE) with gadolinium to assess infarct area, and 3) SPAMM tagging to assess regional wall motion and function. Pictures were taken to show the evaluation of myocardium infarction region samples (Fig 17-18).

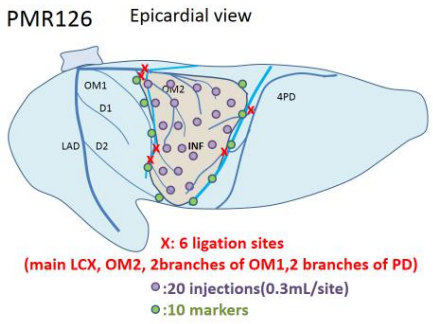

Figure 16 PMR126 Epicardiual view.

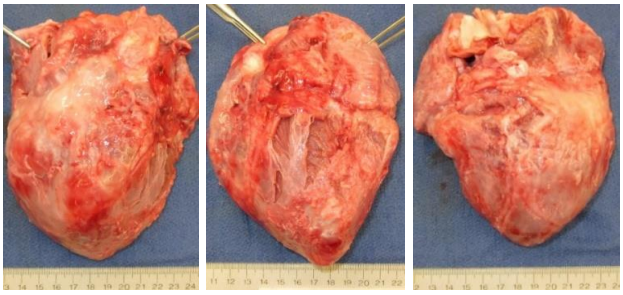

Figure 17 PMR126 Terminal. From left to right: anterior, left lateral and posterior.

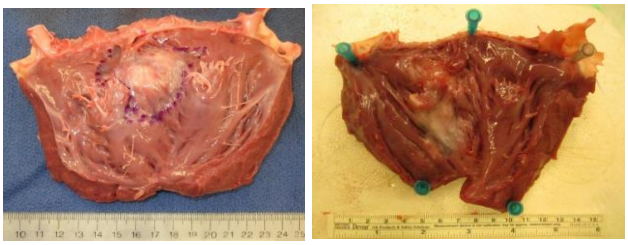

Figure 18 left: PMR126 Infarct size 18.8% (LV areal 8250mm^2, infarct area 1550mm^2) Right: MEP13 Infarct size 16.78% (LV 8022mm^2, infarct area 1346mm^2)

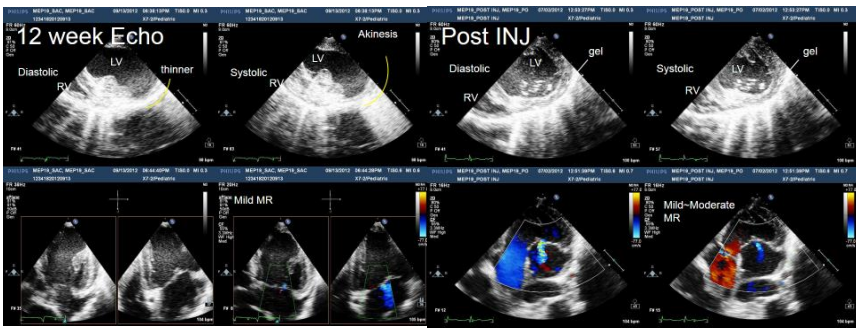

Figure 19 Echocardiographic images of MEP19 sample at 12 weeks scan.

Finite element model

The model used in this study was built by a commercial mesh generate software, TrueGrid (XYZ Scientific, Inc., Livermore, CA, USA). By using the contour points from the MRI data, LV was generated at early diastolic state. Each FE model built based on the contour data got from the experimental data. And the distance from the cap to the

bottom of the model was varies from 5 cm to 6.4 cm which dependents on the scan range set from MRI. After importing the edge surface data of endocardium and epicardium from MRI, the base was fitted to the experimental LV. Figure 20 shows the epicardium and endocardium surfaces build from the surface data from MRI. Then the software could fill up the volume between endocardium and epicardium with elements. These elements represent the myocardium and MI. The finite element model was a 3-D model, consisting of three dimensions which were longitudinal, circumferential and transmural respectively. Each direction had its numbers of elements which was same numbers in each sample model. The model has 12 elements along longitudinal direction, 36 elements along circumferential direction and 3 elements along transmural direction. The fiber angles were assigned to finite element model through a custom MATLAB script. For the remote region from epicardium to endocardium, the fiber angle were assigned from -37° to 83° (Fig 21). The parameterization of the fiber angles in the infarction region were determined from the optimization scheme. In this study, fiber angle search range was set to be -50° to 0° in epicardium and 50° to 90° in endocardium respectively (Fig 21).

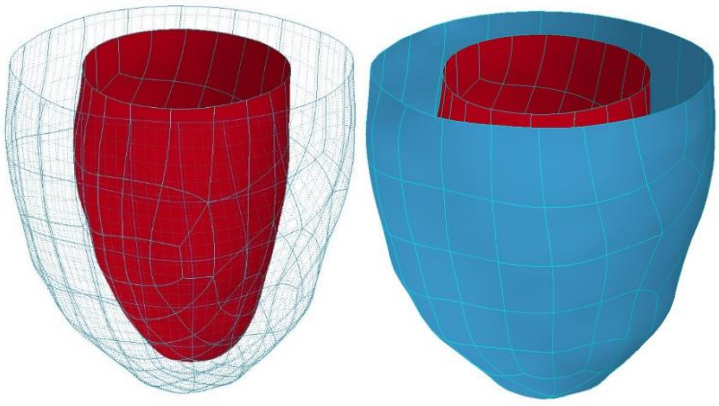

Figure 20 Capture from LS-Prepost of surfaces in LV.

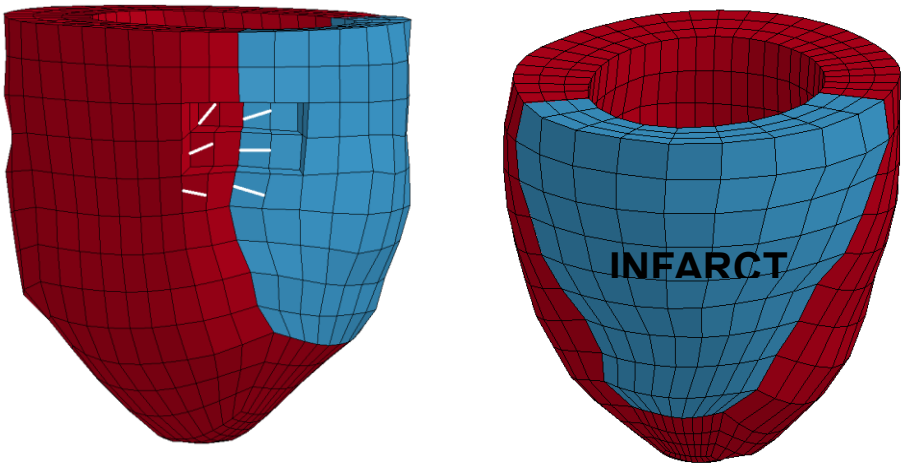

Figure 21 Fiber angle orientation from endocardium to epicardium and infarct region.

Results

The optimization process was performed by a commercial software LS-OPT (Livemore Software Technology Corporation, Livemore, CA). LS-OPT is a standalone design optimization and probabilistic analysis package with an interface to LS-DYNA. The design changes based on experience and this design approach not always lead to the desired result, but it lead to a "best" design. LS-OPT provides a simulation environment that allows distribution of simulation jobs across multiple processors. The optimization process begin with a random initial point and narrow down the design space to get the best result. The design space is governed by the passive parameters in the remote region (4 parameters), the passive parameters in the infarct region (4 parameters), and the MI fiber angles (2 parameters). The optimization algorithm used to minimize the results range was a genetic algorithm (GA). The optimization compared simulation and experimental strain, with a constraint to have the simulation match the measured volume within plus and minus 8%. GA is also called a metaheuristic and it belong to the large class

of evolutionary algorithms. There were 30 iterations used during the optimization, with 100 simulations conducted per iteraton. Thirty iterations took almost 20 hours to get the final result. Six 1 week samples, five 4 week samples and four 8 week samples were been through 30 iterations simulation before get the best results (Table 4-6).

The optimization was seeking to determing the following: C, B_f, B_t, and B_{fs} were parameters of remote region and C_I, B_f_I, B_t_I, and B_{fs}_I were parameters of infarct region. These table also showed epicardium angle, endocardium angle and MSE (mean squared error). In order to determine the influences in treated myocardium wall, plot of biaxial testing results were represents clearly below. Figure 22-23 show the average stiffness changed during the post-MI time course for both the remote and treated MI with hydrogel injections.

Table 4 Parameter values of six 1 week samples from optimization.

1wk	MEP13	MEP17	MEP19	pmr127	pmr126	pmr130
C (hPa)	1.338	1.236	9.141	8.385	4.821	2.94739
Bf	42.44	57.08	3.904	74.32	22.24	55.8006
Bt	41.31	2.346	49.17	1.532	32.29	23.5864
Bfs	48.36	38.56	24.74	49.02	38.24	46.1552
C_I (hPa)	89.36	59.01	9.904	27.58	14.44	58.3569
Bf_I	208.6	212.1	245.1	71.05	244.9	200.023
Bt_I	2.603	26.71	13.91	11.36	14.27	4.11997
Bfs_I	7.798	18.3	14.68	56.44	13.03	6.90619
epiangle	-5.563	-49.68	-1.094	-1.294	-3.672	-0.01684
endoangle	40.5	43.17	40.34	61.63	66.61	75.7309
MSE	5.418	9.077	7.694	4.985	4.671	6.79207

Table 5 Parameter values of five 4 week samples from optimization.

4wk	MEP13	MEP17	pmr130	pmr126	pmr129
C (hPa)	5.716	1.064	12.98	65.22	4.373
Bf	55.03	89.48	54.58	1.004	38.32
Bt	23.83	45.24	3.159	28.87	23.11
Bfs	49.2	47.44	49.89	4.869	46.58
C_I (hPa)	12.68	133.6	20.61	59.06	21.88
Bf_I	204.6	58.58	64.13	45.39	238.9
Bt_I	11.52	2.7	9.473	6.392	20.27
Bfs_I	57.52	1.219	42.44	5.779	13.72
epiangle	-11.11	-2.088	-2.269	-3.062	-0.3384
endoangle	49.56	46.32	26.12	25.55	48.66
MSE	5.718	7.062	7.118	6.644	3.983

Table 6 Parameter values of four 8 week samples from optimization.

8wk	pmr126	pmr128	pmr130	pmr131
C (hPa)	3.655	5.646	12.38	4.203
Bf	86.25	13.13	49.47	28.51
Bt	39.67	11.72	6.32	31.89
Bfs	46.2	49.17	49.11	48.24
C_I (hPa)	10.07	11.38	7.61	2.793
Bf_I	60.33	224.1	177	227.3
Bt_I	13.78	5.447	7.43	59.72
Bfs_I	22.4	11.57	7.461	59.69
epiangle	-0.2211	-0.3513	-2.185	-0.5784
endoangle	0.5581	35.42	27.88	45.62
MSE	10.51	10.02	15.9	4.068

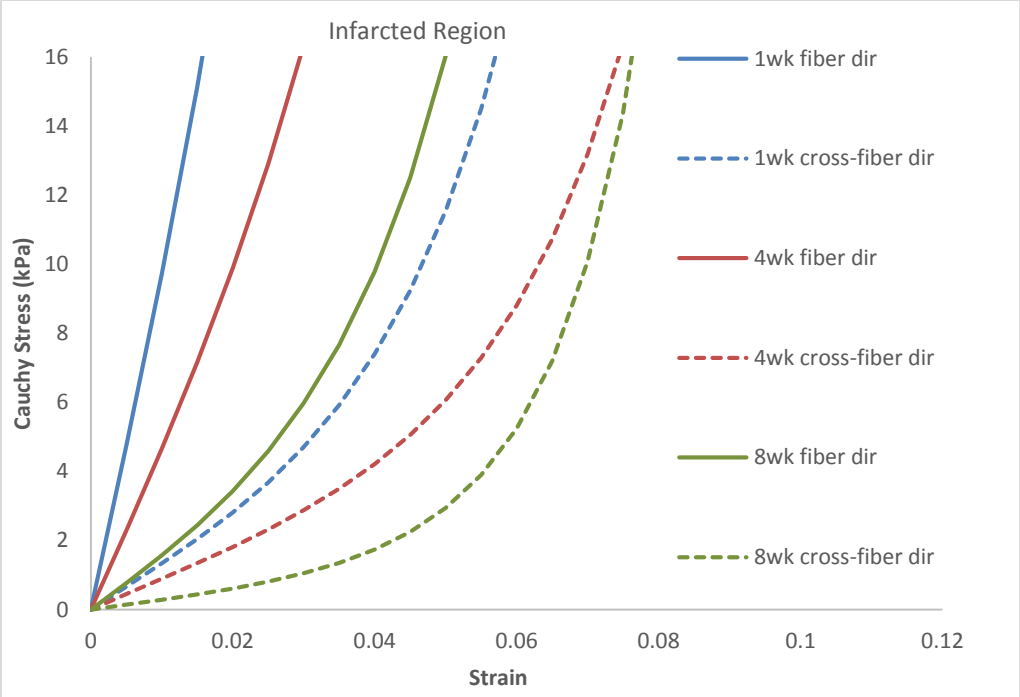

Figure 22 Plot of infarct region stiffness get from simulated biaxial tests of six 1week samples, five 4week samples and four 8week samples.

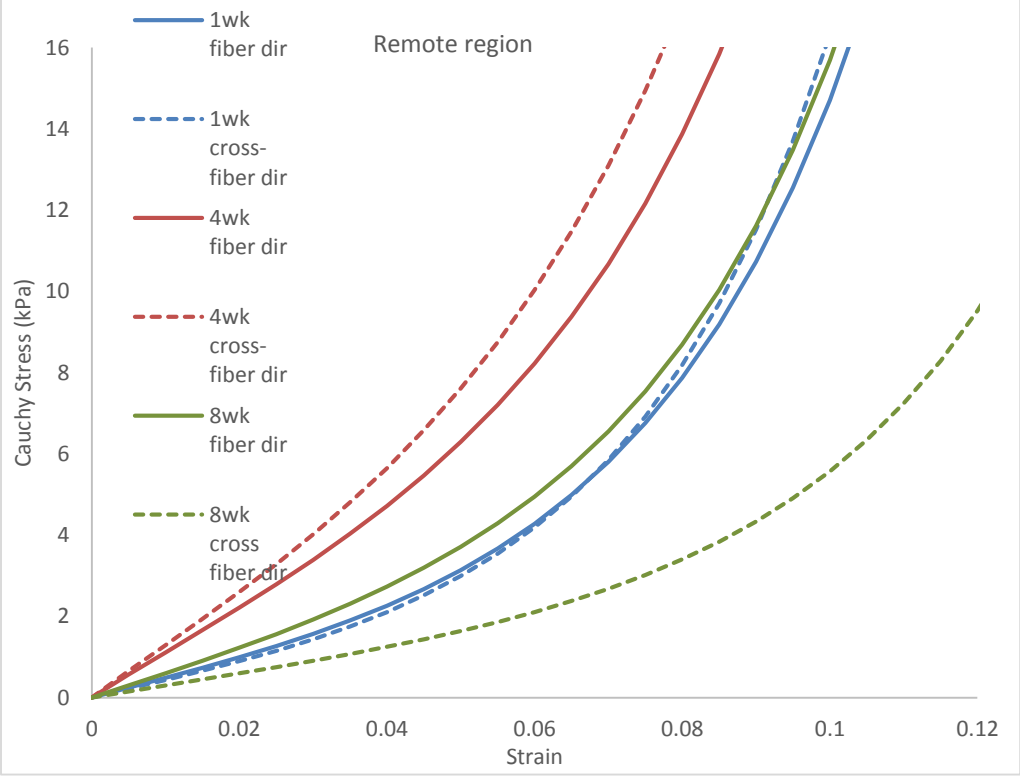

Figure 23 Plot of infarct region stiffness get from simulated biaxial tests of six 1week samples, five 4week samples and four 8week samples.

In order to see the influence during the process, plots were generated for each time point (Fig 24-26).

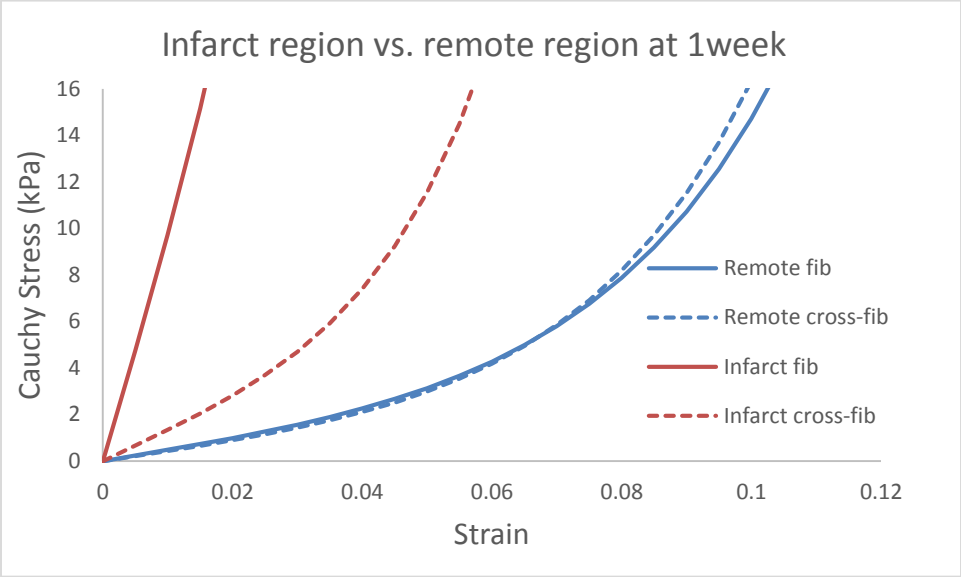

Figure 24 Plot of stiffness in infarct region and remote region at 1 week.

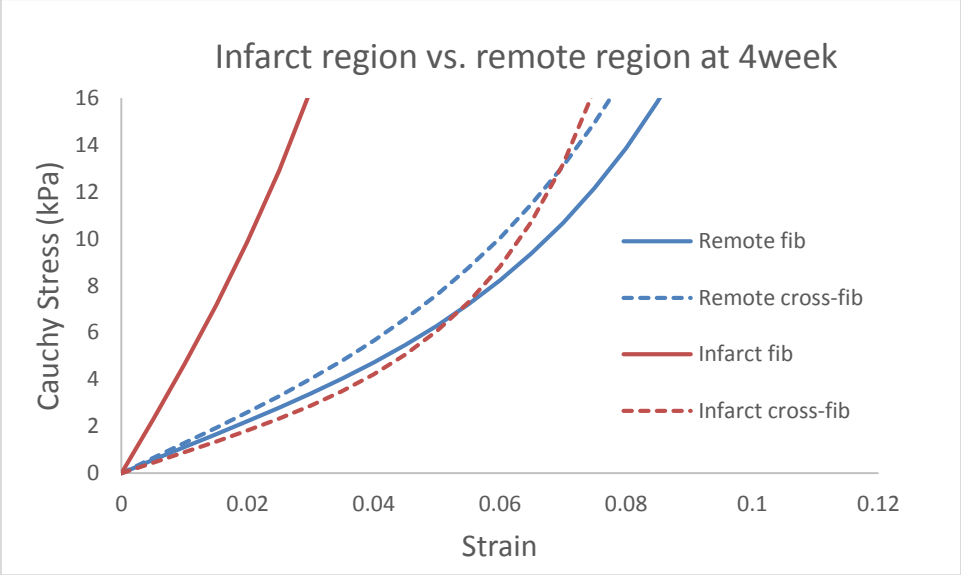

Figure 25 Plot of stiffness in infarct region and remote region at 4 week

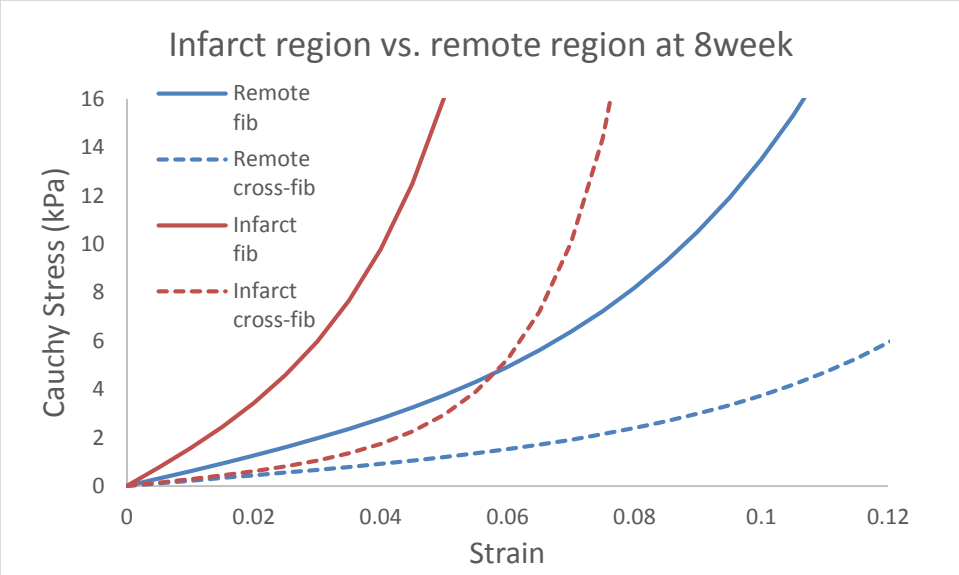

Figure 26 Plot of stiffness in infarct region and remote region at 8 week

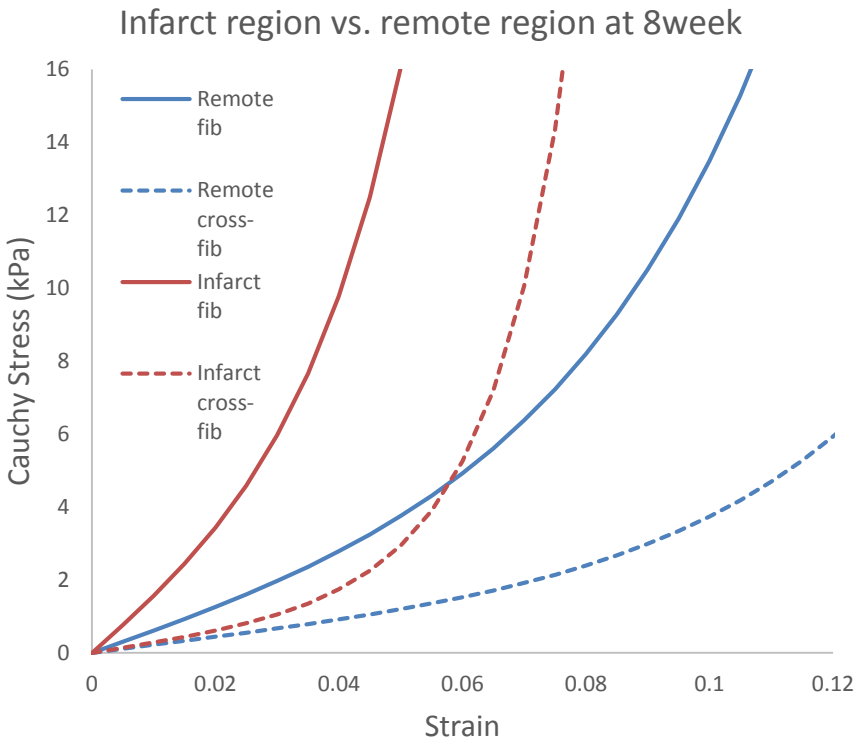

Figure 27 Biaxial results of 8 week infarct region and 8 week remote region on treated cases.

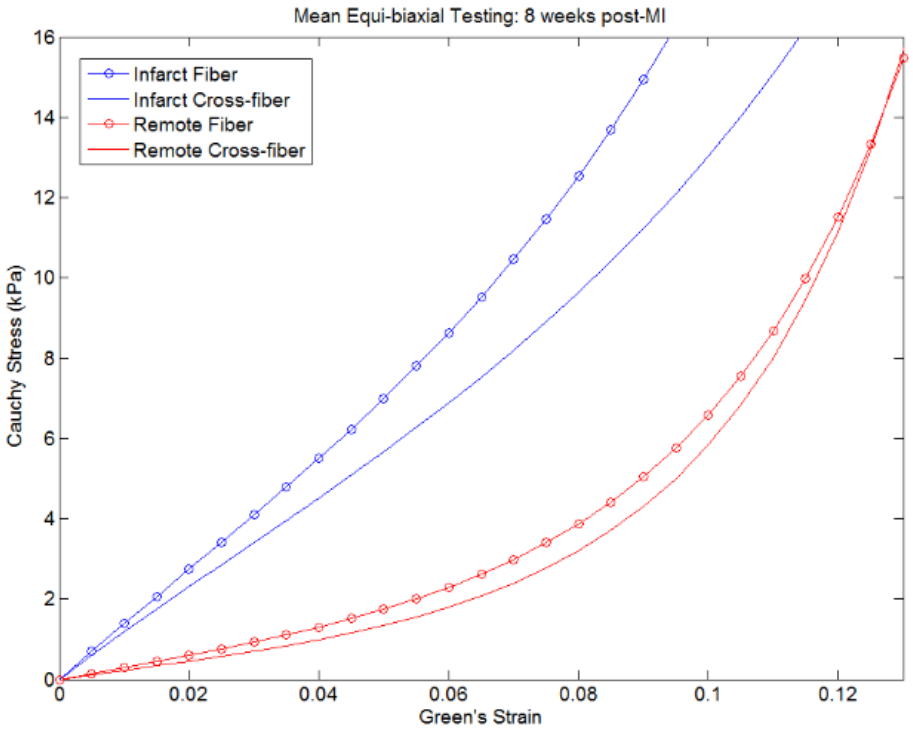

Figure 28 Biaxial results of 8 week infarct region and 8 week remote region on control cases.

The material parameter data was obtained from optimizations by using LS-OPT. Curves were plotted by using a simulated biaxial extension test coded in a custom Matlab script and the averaged stresses (fiber stress and cross-fiber stress) are shown. Material parameters C, B_f, and B_t, were plugged into Eq 9 and Eq 10 to calculate the stiffness in infarct region and parameters C_I, B_f_I, and B_t_I were used to calculate remote region stiffness. Figure 27 showed the compared biaxial test result in both infarct region and remote region at 8 weeks on treated cases. In additional, according to the thesis work done by Mojsejenko, Figure 28 represented the average stress-strain data at 8 weeks on control cases (untreated infarct). It can be seen that the treated infarct is much stiffer than the untreated infarct at 8 weeks post-MI. This means the hydrogel is able to maintain higher stiffness for a longer period of time.

Discussion

This work was used to determine the changes to in-vivo material properties of a myocardium infarction over a serial time course. In the previous studies, FE modeling was used to determine the deformation and contractility of LV wall caused by myocardium infarction. A method for estimating the contractility during heart failure was developed by Sun et al, from the tagged MRI, myocardial strain, LV volume and LV FE model were calculated [43]. Wenk et al. also use this method to develop an FE model to study a sheep with posterolateral infarction [44]. However, the focus of the current work was on the passive properties of the myocardium and infarct tissue.

Table 4-6 obtained from LS-OPT to investigate the material parameter values at 1 week, 4 week and 8 week. As seen from those optimization results, the parameters for infarcted region were significantly higher than remote region. Specifically, the value of B_{f_I} was not only higher than B_f, but also much higher than B_t and B_{fs}. That means hydrogel injections will cause a high stiffness along fiber direction compared to remote region and cross-fiber direction.

Biaxial stress results were calculated by a Matlat script. As seen from results of Figure 22-23, it can be seen clearly that the stiffness increased significantly in infarcted region than remote region due to the hydrogel injection. And then the stiffness become decreased over the time of remodeling process at 4week and 8week. It is clearly to see the increased stiffness at 1 week from Figure 24. This result indicated that hydrogel injections can be used to treat infarcted heart to reduce the onset of MI bulging during

contraction. At 4 weeks, Figure 25 showed that the stiffness still stiffer in infarcted region than the remote region, but there was a reduce trend in anisotropy compared to it at 1 week. That means the stiffness of infarcted region was decreased before 4 week study. As the stiffness decreased over time, however as seen from figure 26, the stiffness still higher in infarcted region compared to the remote region in treated heart at 8 weeks. The Hydrogel had the most influence at the initial phase of myocardium infarction, and the anisotropy was much bigger than 4 weeks and 8 weeks. Figure 27 and Figure 28 represented an average stress-strain curves comparison between the treated cases and control cases at 8 weeks. The trend of curves indicated that the stiffness was higher in treated cases than the control cases, that was because the effect of hydrogel injections.

It is important to observe stiffness changes in LV wall. That was because after the myocardium infarction occurred, the infarcted tissue died. Then tissue become thinner and lose contractility. When high pressure loaded into LV, the thinner infarcted tissue could not resist the load. Hydrogel injection could make the infarct tissue stiffer than remote tissue and also make the LV wall thicker. Also, it could reduce stretching and stress around the infarct region. This is beneficial to prevent dilation of the LV over the time of the remodeling process during myocardium infarction. Another important factor was that before dilation of LV, mitral valve was closed to make sure that the blood could pump into the body and would not flow back into the atrium. After MI, high pressure in LV could make mitral valve open and leak blood so that it would cause a terrible interruption in pumping blood function.

There are a wide range of injection therapies that can be used for myocardial infarct tissue. By using this method, future studies can find better hydrogel composite injection design based on this study. Future studies will add more design of hydrogel injections shape, numbers and material. Also instead of just focusing on the LV, more studies need to have research on the right ventricle. Finally, there could be additional studies to see if there is a better algorithm instead of genetic algorithm to optimize the material properties during the optimization.

CHAPTER 4

Conclusions

To treat cardiovascular disease, medical data was used to create realistic virtual representations of the LV and then utilize predictive computational modeling to improve diagnostic and treatment strategies. By using the contour data from MRI and biaxial testing, finite element models were generated for determining material parameters and the geometry of hydrogel composite injection. Hydrogel injected into a MI could increase the stiffness of the LV wall, thus decreasing bulging during contraction that leads to inefficient ejection. By altering the material parameters with hydrogel injections, myofiber stress and strain were obtained. This information can be used to generate better treatment for the reduction of adverse remolding after myocardium infarction. This study provide insight on how to optimize material parameters to alter the stiffness during LV remolding, and reduce stress on myofibers.

References

1. Nelson, D.M., et al., *Intra-myocardial biomaterial injection therapy in the treatment of heart failure: Materials, outcomes and challenges.* Acta Biomater, 2011. **7**(1): p. 1-15.
2. Costa, K.D., J.W. Holmes, and A.D. McCulloch, *Modelling cardiac mechanical properties in three dimensions.* Philosophical Transactions of the Royal Society of London Series a-Mathematical Physical and Engineering Sciences, 2001. **359**(1783): p. 1233-1250.
3. Demiray, H., *Stresses in Ventricular Wall.* Journal of Applied Mechanics-Transactions of the Asme, 1976. **43**(2): p. 194-197.
4. Humphrey, J.D. and F.C. Yin, *On constitutive relations and finite deformations of passive cardiac tissue: I. A pseudostrain-energy function.* J Biomech Eng, 1987. **109**(4): p. 298-304.
5. Guccione, J.M., A.D. McCulloch, and L.K. Waldman, *Passive material properties of intact ventricular myocardium determined from a cylindrical model.* J Biomech Eng, 1991. **113**(1): p. 42-55.
6. Costa, K.D., et al., *A three-dimensional finite element method for large elastic deformations of ventricular myocardium: II--Prolate spheroidal coordinates.* J Biomech Eng, 1996. **118**(4): p. 464-72.
7. Holzapfel, G.A. and R.W. Ogden, *Constitutive modelling of passive myocardium: a structurally based framework for material characterization.* Philos Trans A Math Phys Eng Sci, 2009. **367**(1902): p. 3445-75.
8. Streeter, D.D., Jr., et al., *Fiber orientation in the canine left ventricle during diastole and systole.* Circ Res, 1969. **24**(3): p. 339-47.
9. Carew, T.E. and J.W. Covell, *Fiber orientation in hypertrophied canine left ventricle.* Am J Physiol, 1979. **236**(3): p. H487-93.
10. Guccione, J.M., et al., *Residual stress produced by ventricular volume reduction surgery has little effect on ventricular function and mechanics: a finite element model study.* J Thorac Cardiovasc Surg, 2001. **122**(3): p. 592-9.
11. Starling, R.C., et al., *Sustained benefits of the CorCap Cardiac Support Device on left ventricular remodeling: three year follow-up results from the Acorn clinical trial.* Ann Thorac Surg, 2007. **84**(4): p. 1236-42.
12. Klodell, C.T., Jr., et al., *Worldwide surgical experience with the Paracor HeartNet cardiac restraint device.* J Thorac Cardiovasc Surg, 2008. **135**(1): p. 188-95.
13. Blom, A.S., et al., *Infarct size reduction and attenuation of global left ventricular remodeling with the CorCap (TM) stop cardiac support device following acute myocardial infarction in sheep.* Heart Failure Reviews, 2005. **10**(2): p. 125-139.
14. Fukamachi, K. and P.M. McCarthy, *Initial safety and feasibility clinical trial of the myosplint device.* J Card Surg, 2005. **20**(6): p. S43-7.
15. Kashem, A., et al., *Early and late results of left ventricular reshaping by passive cardiac-support device in canine heart failure.* J Heart Lung Transplant, 2003. **22**(9): p. 1046-53.

16. Blom, A.S., et al., *Infarct size reduction and attenuation of global left ventricular remodeling with the CorCap cardiac support device following acute myocardial infarction in sheep.* Heart Fail Rev, 2005. **10**(2): p. 125-39.
17. Kichula, E.T., et al., *Experimental and Computational Investigation of Altered Mechanical Properties in Myocardium after Hydrogel Injection.* Ann Biomed Eng, 2013.
18. Guccione, J.M., L.K. Waldman, and A.D. McCulloch, *Mechanics of active contraction in cardiac muscle: Part II--Cylindrical models of the systolic left ventricle.* J Biomech Eng, 1993. **115**(1): p. 82-90.
19. Wenk, J.F., et al., *A method for automatically optimizing medical devices for treating heart failure: designing polymeric injection patterns.* J Biomech Eng, 2009. **131**(12): p. 121011.
20. Wenk, J.F., et al., *A Method for Automatically Optimizing Medical Devices for Treating Heart Failure: Designing Polymeric Injection Patterns.* Journal of Biomechanical Engineering-Transactions of the Asme, 2009. **131**(12).
21. Tozeren, A., *Continuum Rheology of Muscle-Contraction and Its Application to Cardiac Contractility.* Biophysical Journal, 1985. **47**(3): p. 303-309.
22. Guccione, J.M., K.D. Costa, and A.D. McCulloch, *Finite element stress analysis of left ventricular mechanics in the beating dog heart.* J Biomech, 1995. **28**(10): p. 1167-77.
23. Astolfi, D., et al., *[Surgical treatment of aortic supravalvular stenosis. Long-term results after more than 1 year].* G Ital Cardiol, 1973. **3**(2): p. 176-85.
24. Yin, F.C., et al., *Quantification of the mechanical properties of noncontracting canine myocardium under simultaneous biaxial loading.* J Biomech, 1987. **20**(6): p. 577-89.
25. Demer, L.L. and F.C. Yin, *Passive biaxial mechanical properties of isolated canine myocardium.* J Physiol, 1983. **339**: p. 615-30.
26. Ifkovits, J.L., et al., *Injectable hydrogel properties influence infarct expansion and extent of postinfarction left ventricular remodeling in an ovine model.* Proc Natl Acad Sci U S A, 2010. **107**(25): p. 11507-12.
27. Walker, J.C., et al., *MRI-based finite-element analysis of left ventricular aneurysm.* Am J Physiol Heart Circ Physiol, 2005. **289**(2): p. H692-700.
28. Morita, M., et al., *Modification of infarct material properties limits adverse ventricular remodeling.* Ann Thorac Surg, 2011. **92**(2): p. 617-24.
29. Jacobs, N.T., et al., *Effect of orientation and targeted extracellular matrix degradation on the shear mechanical properties of the annulus fibrosus.* J Mech Behav Biomed Mater, 2011. **4**(8): p. 1611-9.
30. Szczesny, S.E., et al., *Biaxial tensile testing and constitutive modeling of human supraspinatus tendon.* J Biomech Eng, 2012. **134**(2): p. 021004.
31. Gupta, V. and K.J. Grande-Allen, *Effects of static and cyclic loading in regulating extracellular matrix synthesis by cardiovascular cells.* Cardiovasc Res, 2006. **72**(3): p. 375-83.
32. Holmes, J.W., T.K. Borg, and J.W. Covell, *Structure and mechanics of healing myocardial infarcts.* Annu Rev Biomed Eng, 2005. **7**: p. 223-53.

33. Engelmayr, G.C., Jr., et al., *Accordion-like honeycombs for tissue engineering of cardiac anisotropy.* Nat Mater, 2008. **7**(12): p. 1003-10.
34. Lee, A.A. and A.D. McCulloch, *Multiaxial myocardial mechanics and extracellular matrix remodeling: mechanochemical regulation of cardiac fibroblast function.* Adv Exp Med Biol, 1997. **430**: p. 227-40.
35. Rappaport, D., et al., *Assessment of myocardial regional strain and strain rate by tissue tracking in B-mode echocardiograms.* Ultrasound Med Biol, 2006. **32**(8): p. 1181-92.
36. Kortsmit, J., et al., *The effect of hydrogel injection on cardiac function and myocardial mechanics in a computational post-infarction model.* Comput Methods Biomech Biomed Engin, 2013. **16**(11): p. 1185-95.
37. Tous, E., et al., *Influence of injectable hyaluronic acid hydrogel degradation behavior on infarction-induced ventricular remodeling.* Biomacromolecules, 2011. **12**(11): p. 4127-35.
38. Xu, C., et al., *Deformation analysis of 3D tagged cardiac images using an optical flow method.* J Cardiovasc Magn Reson, 2010. **12**: p. 19.
39. Thomas, D., et al., *Quantitative assessment of regional myocardial function in a rat model of myocardial infarction using tagged MRI.* MAGMA, 2004. **17**(3-6): p. 179-87.
40. Zhou, R., et al., *Assessment of global and regional myocardial function in the mouse using cine and tagged MRI.* Magn Reson Med, 2003. **49**(4): p. 760-4.
41. Osman, N.F. and J.L. Prince, *Visualizing myocardial function using HARP MRI.* Phys Med Biol, 2000. **45**(6): p. 1665-82.
42. Witschey, W.R., et al., *Rotating frame spin lattice relaxation in a swine model of chronic, left ventricular myocardial infarction.* Magn Reson Med, 2010. **64**(5): p. 1453-60.
43. Sun, K., et al., *A computationally efficient formal optimization of regional myocardial contractility in a sheep with left ventricular aneurysm.* J Biomech Eng, 2009. **131**(11): p. 111001.
44. Wenk, J.F., et al., *Regional Left Ventricular Myocardial Contractility and Stress in a Finite Element Model of Posterobasal Myocardial Infarction.* Journal of Biomechanical Engineering-Transactions of the Asme, 2011. **133**(4).

VITA

Hua Wang was born in Dongying, Shandong, China. After completing her work at high school, in 2008, she entered China University of Mining and Technology, Jiangsu, China. After two years, she joined a 2+2 combined education program that was cosponsored by the University of Kentucky. She received the degree of Bachelor of Science both from University of Kentucky and China University of Mining and Technology in May 2012. Since 2012, she joined the Computational Biomechanics Laboratory, which is run by Dr. Jonathan Wenk to continue Master's degree. During the Master time, she have been the second author of a published paper titled "Experimental and Computational Investigation of Altered Mechanical Properties in Myocardium after Hydrogel Injection" in the ABME jounal.

This thesis was typed by Hua Wang